

Asking like Socrates: Socrates helps VLMs understand remote sensing images

Run Shao^{1,2,*} Ziyu Li^{1,*} Zhaoyang Zhang¹ Linrui Xu¹ Xinran He² Hongyuan Yuan^{1,2}
 Bolei He² Yongxing Dai² Yiming Yan³ Yijun Chen³ Wang Guo¹ Haifeng Li^{1,†}

¹School of Geosciences and Info-Physics, Central South University, Changsha, China

²Baidu Inc., Beijing, China

³School of Earth Sciences, Zhejiang University, Hangzhou, China

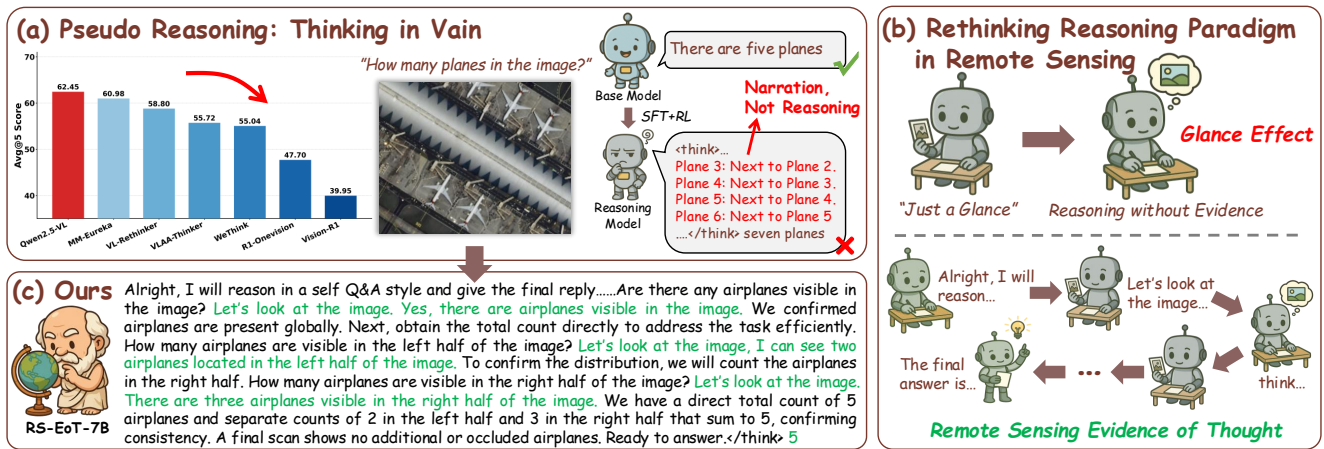


Figure 1. Illustration of the pseudo reasoning problem and our RS-EoT solution. (a) Existing models show pseudo reasoning: explicit thinking (blue bars) degrades performance below the non-reasoning base model (red bar). (b) We attribute this to the “Glance Effect”—reasoning based on a single, coarse perception. We propose RS-EoT, an iterative evidence-seeking loop. (c) Our model, RS-EoT-7B, successfully solves the task by iteratively reasoning and seeking visual evidence.

Abstract

Recent multimodal reasoning models, inspired by DeepSeek-R1, have significantly advanced vision–language systems. However, in remote sensing (RS) tasks, we observe widespread pseudo reasoning: models narrate the process of reasoning rather than genuinely reason toward the correct answer based on visual evidence. We attribute this to the Glance Effect, where a single, coarse perception of large-scale RS imagery results in incomplete understanding and reasoning based on linguistic self-consistency instead of visual evidence. To address this, we propose RS-EoT (Remote Sensing Evidence-of-Thought), a language-driven, iterative visual evidence-seeking paradigm. To instill this paradigm, we propose SocraticAgent, a self-play multi-agent system that synthesizes reasoning traces

via alternating cycles of reasoning and visual inspection. To enhance and generalize these patterns, we propose a two-stage progressive RL strategy: first, RL on fine-grained Grounding tasks to enhance RS-EoT capabilities, followed by RL on RS VQA to generalize to broader understanding scenarios. Experiments show RS-EoT achieves state-of-the-art performance on multiple RS VQA and grounding benchmarks. Analyses reveal clear iterative cycles of reasoning and evidence seeking, confirming RS-EoT mitigates the Glance Effect and enables genuine evidence-grounded reasoning. Our code, data, and models are available at https://geox-lab.github.io/Asking_like_Socrates.

1. Introduction

Recent deep reasoning models, such as DeepSeek-R1 [8], Qwen3 [41], and Doubao-Seed-1.6 [2], show the SFT–RL

*Equal contribution.

†Corresponding author.

paradigm substantially enhances long-chain reasoning [10, 23, 32, 39], enabling breakthroughs in math, code, and agent planning. This paradigm was then extended to multi-modal settings, training vision–language models to generate structured reasoning [3, 10, 23, 34, 42, 43]. This progress has significantly advanced multimodal systems, stimulating interest in applying deep reasoning to complex visual domains [19, 25, 30, 45, 47].

However, owing to the unique properties of remote sensing (RS) imagery, such as wide spatial extents, large scale variations, and sparse and subtle visual clues, these models often exhibit *pseudo reasoning* [15, 30] in RS tasks (Fig. 1-a). Despite producing explicit reasoning chains, their performance on RS tasks shows no gain [3, 6, 7, 28], and even degrades compared to the base model. In other words, they merely *describe* a reasoning process rather than *performing* one. We attribute this to the *Glance Effect* (Fig. 1-b). Current models perform only a single, coarse perception pass (a “glance”) before reasoning. This is insufficient, leading to reasoning built on incomplete visual evidence. Consequently, the model drifts toward linguistically self-consistent narratives rather than evidence-based logic, which can even degrade performance.

This suggests RS reasoning requires iterative, not static, evidence acquisition [18, 30]. Human analysts exemplify this, using repeated cycles of inspection and refinement. To emulate this, models must adopt a paradigm where reasoning guides perception to dynamically seek new visual evidence, rather than relying on a fixed initial view.

To this end, we propose *RS-EoT (Remote Sensing Evidence-of-Thought)*, a language-driven iterative evidence-seeking reasoning paradigm. It frames reasoning as a reasoning–perception loop where the model continuously revisits the image, seeking new visual cues guided by the evolving reasoning. Thus, perceptual grounding is progressively refined, not fixed at the outset. To instill RS-EoT, we follow Deepseek-R1’s methodology: first, Supervised Fine-Tuning (SFT) cold-starts the reasoning mode, and then Reinforcement Learning (RL) enhances and generalizes these patterns. [8, 10, 23, 43].

In the SFT phase, we propose a novel data synthesis method called *SocraticAgent* to equip the model with the aforementioned self-iterative evidence-seeking capability. Inspired by the Socratic Method, which fosters knowledge acquisition through a step-by-step questioning process rather than direct instruction, we design *SocraticAgent* as a self-play multi-agent system to synthesize RS-EoT reasoning traces. Specifically, *SocraticAgent* contains a Reasoner and a Perceiver. The former is responsible for pure-language reasoning and posing perceptual questions about the image as necessitated by the reasoning, while the latter is responsible for perceiving the image and answering the questions posed by the Reasoner. They engage in a multi-

turn dialogue, simulating the iterative reasoning–perception loop. Through a Socratic self-play strategy, wherein each agent is prompted with the presumed limited capability of the other, the Reasoner is guided to pose simple, incremental questions and the Perceiver to return accurate yet concise results, ensuring detailed and progressive traces. This synthesis method yielded the RS-EoT-4K dataset, which is used for the initial SFT cold-start to instill this self-iterative evidence-seeking reasoning in the model.

In the RL stage, we propose a two-stage progressive training pipeline to further enhance and generalize the RS-EoT capability. First, adhering to the principle that “iron sharpens iron,” we perform RL on fine-grained grounding tasks, which are precisely those that most demand fine-grained visual evidence, to specifically enhance the RS-EoT capability. Building on this foundation, we then conduct RL on general RS VQA tasks to generalize this capability to broader remote sensing scenarios. However, considering that existing RS VQA data is often simple (*e.g.*, Yes/No types), it is highly susceptible to reward hacking and thus unsuitable for RL training. To address this, we propose a multiple-choice VQA reconstruction strategy and a tailored reward function, enabling stable RL training.

Experiments show RS-EoT achieves state-of-the-art performance on multiple RS VQA and grounding benchmarks. Case studies and attention analyses confirm the model employs clear iterative cycles of reasoning and evidence seeking, validating the effectiveness of RS-EoT.

Our main contributions are summarized as follows:

- We propose **RS-EoT** (Remote Sensing Evidence-of-Thought), a language-driven iterative evidence-seeking reasoning paradigm for remote sensing.
- We introduce a complete framework to instill this paradigm: (1) **SocraticAgent** to synthesize the **RS-EoT-4K** dataset for SFT cold-starting. (2) A two-stage **progressive Grounding+VQA RL** strategy, featuring a novel VQA data reconstruction method that enables stable RL training on simple RS VQA datasets.
- We train **RS-EoT-7B**, which achieves SOTA on multiple RS VQA and grounding benchmarks. Analyses confirm it mitigates the Glance Effect via clear iterative reasoning and evidence-seeking cycles.

2. Related Work

2.1. Vision-language Model for Remote Sensing

The automated interpretation of RS images is crucial for applications like environmental monitoring, urban planning, and disaster response [11, 18]. This has spurred development of VLMs for RS, with models like GeoChat [14], Sky-sense [9], and RingmoGPT [36] demonstrating strong image understanding capabilities. More recently, the field has advanced toward complex reasoning, with models like Geo-

R1 [40] and VHM-RL [13] adopting the SFT-RL paradigm to output explicit reasoning chains.

However, a key issue persists: these models often rely on a single-pass, global perception, neglecting detailed information and regional cues. This is particularly problematic for RS images with their wide geographical ranges and large scale variations. In contrast, our work introduces RS-EoT, an iterative evidence-seeking paradigm that replaces this single-pass approach with a dynamic loop of linguistic deduction and targeted visual inspection.

2.2. Large Language Reasoning Model

Reasoning in LLMs was reshaped by the Chain-of-Thought (CoT) paradigm [37], which showed that eliciting multi-step traces improves complex reasoning. This inspired variants like Least-to-Most [50], Program-of-Thought [4], and advanced models like OpenAI’s o1 [12]. A pivotal development is the SFT-RL paradigm, popularized by DeepSeek-R1 [8]. This approach uses SFT to cold-start reasoning patterns, then applies RL to refine and generalize them. Algorithms like Group Relative Policy Optimization (GRPO) [27] and its variants [39, 44] offer more stable optimization for long-sequence reasoning than PPO [26]. Our methodology builds upon this SFT-RL paradigm: we first employ SFT to cold-start the iterative evidence-seeking pattern, then utilize a two-stage progressive RL process to enhance and generalize this capability.

2.3. Multimodal reasoning model

The SFT-RL paradigm was rapidly adopted in multimodal learning, spawning models like Vision-R1 [10], WeThink [42], and R1-OneVision [43]. These models, with subsequent refinements [3, 23, 34], transferred this methodology to visual-language contexts. However, they largely inherit language-oriented patterns, assuming reasoning can occur over a static, global visual representation. This assumption fails in remote sensing, where tasks demand iterative, region-specific inspection.

To address this gap, we propose RS-EoT, an iterative, evidence-seeking paradigm tailored for remote sensing. We introduce a complete framework to instill this capability, featuring: (1) a Socratic-inspired mechanism to synthesize RS-specific reasoning traces, and (2) a multi-stage progressive training pipeline to instill this behavior. This design overcomes the limitations of single-pass, language-oriented reasoning frameworks.

3. Method

We aim to enable multimodal models to perform evidence-seeking reasoning over remote sensing imagery. To this end, we first introduce **RS-EoT (Remote Sensing Evidence-of-Thought)**, which characterizes the desired reasoning pattern for remote sensing: reasoning is

language-driven, iteratively seeking visual evidence to refine the reasoning chain and ultimately converge on the correct answer. Following the Deepseek-R1, we first inject the RS-EoT reasoning mode via SFT cold-starting, and then enhance and generalize it through RL. An overview of our method is presented in Fig. 2.

To instill this reasoning pattern, a primary challenge is synthesizing the cold-start data. To this end, we propose **SocraticAgent**, a self-play multi-agent system that synthesizes RS-EoT reasoning traces. SocraticAgent simulates an iterative process of reasoning (via a Reasoner) and visual evidence seeking (via a Perceiver), ensuring each reasoning step is grounded in verifiable visual evidence. These synthesized traces are then used for SFT to cold-start the RS-EoT reasoning mode.

Building on this SFT foundation, we adopt a **two-stage progressive RL** strategy to further enhance and generalize this capability. The first stage performs RL on fine-grained grounding tasks. Since these tasks naturally demand iterative evidence seeking, this stage effectively strengthens the RS-EoT behavior learned during SFT. The second stage performs RL on general remote sensing VQA, allowing the learned RS-EoT pattern to generalize to broader RS understanding scenarios. The final model obtained from this process is termed **RS-EoT-7B**.

3.1. SFT: RS-EoT Cold-Start

3.1.1. RS-EoT

The RS-EoT reasoning paradigm is defined by two core principles. First, **reasoning is orchestrated by natural language**, which serves as the primary medium for formulating hypotheses, planning evidence-seeking steps, and refining intermediate conclusions. Language is not merely a description of multimodal information but the active controller that determines when and how to probe for multimodal evidence. Second, **visual information functions as on-demand evidence within the reasoning chain**. Instead of relying on a single, static global perception, the model actively seeks, verifies, and integrates localized visual evidence at each reasoning step. Through this iterative loop of language-driven reasoning and targeted evidence retrieval, RS-EoT enables more faithful, interpretable, and evidence-grounded decision-making in remote sensing tasks.

3.1.2. Asking like Socrates

A core challenge is *how to synthesize RS-EoT reasoning traces from scratch*, given that existing models do not possess this reasoning mode. We draw inspiration from the Socratic method, which encourages knowledge discovery through a structured process of questioning rather than direct instruction, proposing that the iterative process of reasoning and evidence seeking can be framed as a continuous, incremental process of inquiry.

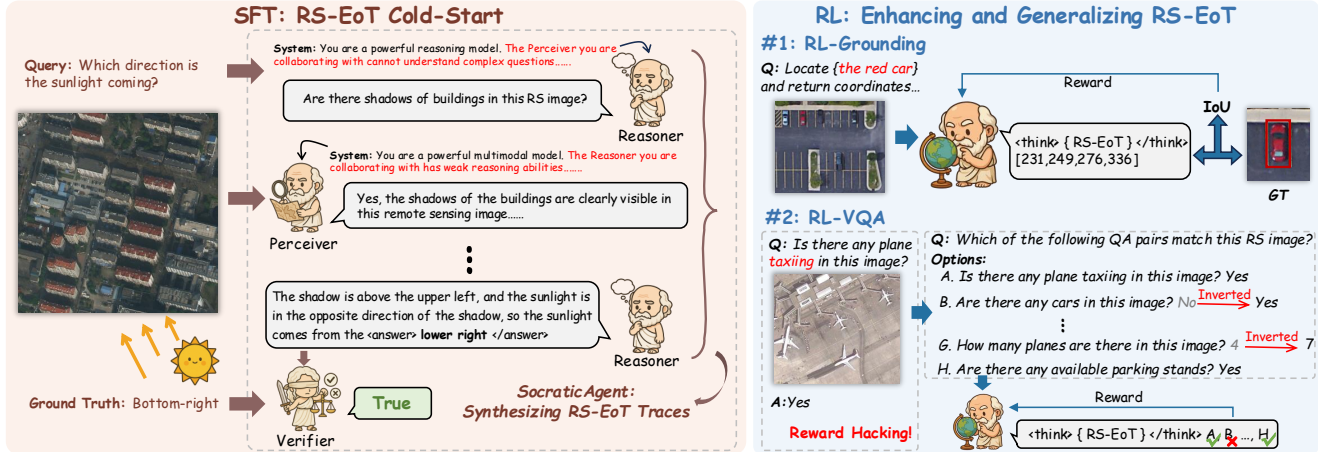


Figure 2. Overview of our method to instill the RS-EoT paradigm. **(Left) SFT: RS-EoT Cold-Start:** We propose SocraticAgent to synthesize reasoning traces. A Reasoner (text-only) and a Perceiver (image-aware) engage in an iterative dialogue, guided by a self-play prompting mechanism. **(Right) RL: Enhancing and Generalizing RS-EoT:** A two-stage progressive RL pipeline. Stage 1 (RL-Grounding) enhances fine-grained evidence-seeking via an IoU-based reward. Building on this, Stage 2 (RL-VQA) generalizes reasoning by converting simple VQA datasets into a multiple-choice format with a graded reward for stable training.

For instance, when addressing the problem, “What is the heading of the ship in this remote sensing image?” one might first naturally ask, “Is there a ship in the image?” This is followed by a coarse visual inspection to confirm its presence. Next, one would reason based on common sense: if the ship is moving, its wake might indicate the direction of travel. This hypothesis, derived from reasoning, leads to a new, more specific question: “In which direction is the ship’s wake pointing?” This prompts a detailed visual inspection, and by observing the wake, one can finally infer the ship’s heading (as the opposite direction of the wake).

By emulating this Socratic questioning, an iterative process of posing questions, seeking visual evidence, and refining the reasoning chain, we can progressively correct and complete our logical path to correctly solve the problem. Simulating the aforementioned process, we propose SocraticAgent, a self-play multi-agent system capable of synthesizing RS-EoT reasoning traces from remote sensing VQA datasets. It primarily comprises two roles: the Reasoner and the Perceiver.

- **Reasoner.** Instantiated by GPT-5-mini [24], the Reasoner operates solely on textual queries and basic image metadata (e.g., modality, count, size), lacking direct access to the RS images. It performs pure-text reasoning and is prompted to pose perceptual questions to the Perceiver when visual information is needed. Upon receiving the Perceiver’s answers, it continues to reason or pose further questions until it can formulate a final answer. Throughout the interaction, the Reasoner continuously analyzes, summarizes, and integrates the Perceiver’s feedback to build a coherent semantic understanding, ultimately producing the final answer.

- **Perceiver.** Implemented using a powerful multimodal model (Gemini-2.5-flash [5] in our setup), the Perceiver’s input consists solely of the RS image and the questions posed by the Reasoner, without access to the original task query. Its sole task is to receive the Reasoner’s questions and provide accurate answers based on the remote sensing image.

They engage in a multi-turn dialogue, culminating in the Reasoner providing the final answer. We then introduce a **Verifier** (instantiated by doubao-seed-1.6-thinking [2]) to validate the Reasoner’s answer against the ground truth. The design rationale is: if the Reasoner, despite having no direct visual access, arrives at the correct solution, the intermediate dialogue is deemed a reliable reasoning trace. This dialogue history is then concatenated based on the following template and formatted into a self QA style reasoning trajectory. Fig. 3 illustrates an actual case.

```

SocraticAgent EoT Trace Concatenation Template

<think> Alright, I will reason in a self QA
style and give the final reply.
{Reasoner (round 1): thought & question}
{Perceiver (round 1): response}
...
{Reasoner (round N): thought & question}
{Perceiver (round N): response}
{Reasoner (round N+1): final answer}
</think> {Final answer from Reasoner}

```

3.1.3. Self-play Prompting Mechanism

However, in practice, we found that the Reasoner tends to forgo detailed reasoning, often defaulting to sending the original query directly to the Perceiver, resulting in an overly “jumpy” reasoning process. The Perceiver, in turn,

is prone to returning overly exhaustive visual information, much of it irrelevant to the specific question. This distracts the Reasoner, leading it to produce hasty responses.

Therefore, we designed an elegant self-play prompting mechanism. Specifically, we prompt each agent that its collaborator is “weak”. The Reasoner is told, “The Perceiver you are collaborating with cannot understand complex questions.” The Perceiver is told, “The Reasoner you are collaborating with has weak reasoning abilities.” This strategy forces the Reasoner to perform detailed problem decomposition and pose simple, incremental questions. Concurrently, it compels the Perceiver to provide answers that are accurate yet concise, without extraneous information. This self-play mechanism ensures their multi-turn dialogue converges into a detailed, progressively structured reasoning trace.

Ultimately, we synthesized a multi-modal RS-EoT dataset, termed RS-EoT-4K, (including RGB, infrared, and SAR imagery) for SFT cold-starting. Data statistics and training details are provided in Sec. 4.

3.2. RL: Enhancing and Generalizing RS-EoT

To ensure the model’s RS-EoT reasoning capability is sufficiently powerful, we build upon the SFT stage with a two-stage progressive reinforcement learning pipeline designed to first enhance and subsequently generalize this capability.

3.2.1. Stage#1: Fine-grained Grounding RL

Starting with the SFT model, adhering to the principle that “iron sharpens iron,” we first perform reinforcement learning on fine-grained grounding tasks. These tasks are selected precisely because they most demand fine-grained visual evidence-seeking, thereby specifically strengthening the model’s RS-EoT reasoning capability.

Implementation-wise, we prompt the model to output the target object’s location in the format “[x1, y1, x2, y2]”. We then calculate the Intersection over Union (IoU) with the ground truth and use the IoU score directly as the reward. We also apply a strict format-based reward during this process to ensure output consistency.

3.2.2. Stage#2: General RS VQA RL

To generalize the model’s reasoning to broader RS scenarios, we further perform RL on general RS VQA datasets. However, existing RS VQA datasets predominantly contain *Yes/No* or low-reasoning-intensity questions [16, 21, 22], which are highly susceptible to reward hacking.

To address this, we propose a multiple-choice RL data reconstruction strategy that converts existing simple RS VQA datasets into a format that stably supports RL training. Specifically, we observe that while current RS VQA datasets feature simple questions and answers, they often map a single image to multiple QA pairs (stemming

from their construction process, often being programmatically converted from traditional classification or detection datasets). Leveraging this property, we convert them into multiple-choice questions. Without loss of generality, the reconstruction process for a single sample is as follows:

1. Collect a remote sensing image I and its associated QA set $\{(Q_i, A_i)\}_{i=1}^m$ with $10 < m < 15$.
2. Randomly invert the answers of n QA pairs to create n incorrect QA pairs, for example by changing “Yes” to “No” or adding/subtracting a random integer from a numeric answer, with $1 < n < m$.
3. Formulate a multiple-choice question (MCQ) sample using “Which of the following QA pairs match this remote sensing image?” as the query, and use the m QA pairs as the options.

The following is an example:

Multiple-Choice RL Data Reconstruction Example

Query: <image>Which of the following QA pairs match this remote sensing image?

A. Is there a square in the image? yes

B. Are there cars in the image? no

Inverted; cars are actually present

...

J. How many ships are in the image? 3

K. How many trees are in the image? 7

Inverted; there are actually 4 trees

Ground truth: A, ..., E, J

Reward design. Given the large number of options, the model often cannot produce a perfectly correct answer on this reconstructed data. To avoid training collapse, we design a tailored graded reward function. Specifically, we assign an option-level, equal-weight, symmetric accuracy reward: *selecting a correct option* and *correctly rejecting an incorrect option* both receive a positive reward, whereas *selecting an incorrect option* or *failing to select a correct option* receive zero reward. Let $\mathbf{y} \in \{0, 1\}^N$ denote ground-truth labels (1 = correct, 0 = incorrect) and $\hat{\mathbf{y}} \in \{0, 1\}^N$ the model’s binary choices (1 = chosen, 0 = not chosen). The per-question reward is

$$r_{\text{qa}} = 1 - \frac{1}{N} \sum_{i=1}^N |y_i - \hat{y}_i|. \quad (1)$$

This reward provides a stable, graded training signal by *symmetrically* penalizing both misses and false selections and *equally* weighting all options. This design effectively mitigates reward hacking and necessitates multi-round reasoning with evidence aggregation, forcing the model to verify each distinct option against the visual evidence to maximize its score.

Table 1. Main comparison on remote sensing general VQA and fine-grained grounding. We compare RS-EoT-7B with recent multimodal reasoning models (all based on Qwen2.5-VL-7B) as well as two remote-sensing-oriented reasoning models (Geo-R1 and VHM-RL). RS-EoT-7B consistently achieves the best results across both VQA and grounding tasks, demonstrating the effectiveness of the RS-EoT paradigm in remote sensing scenarios. Abbreviations: VLAA-T = VLAA-Thinker, VL-R = VL-Rethinker, Vis-R1 = Vision-R1, MM-E = MM-Eureka, R1-OV = R1-OneVision.

Benchmark	Metric	RS-EoT-7B	Qwen2.5VL [1]	WeThink [42]	VLAA-T [3]	VL-R [34]	Vis-R1 [10]	MM-E [23]	R1-OV [43]	Geo-R1 [40]	VHM-RL [13]
<i>Remote Sensing General QA</i>											
RSFG-VQA [22]	Avg@5	67.85	62.45	55.04	55.72	58.80	39.95	60.98	47.70	45.03	53.04
	Conv@5	68.90	62.46	41.07	37.87	57.88	41.94	60.82	48.00	39.76	51.06
	Pass@5	85.28	77.16	61.43	77.88	76.37	57.81	71.22	77.66	71.96	61.56
RSFG-SC [22]	Scene@acc	64.05	57.42	60.12	56.50	58.82	21.63	56.98	47.04	52.46	64.90
	Object@F1	56.52	36.78	38.35	32.91	34.84	6.27	31.57	24.65	20.82	30.89
VRSBench [17]	Avg@5	63.09	62.45	62.17	60.54	55.04	37.72	55.25	44.59	57.00	57.01
	Conv@5	64.12	62.58	62.36	61.16	55.49	37.39	55.37	46.36	58.65	56.76
	Pass@5	83.54	75.62	73.84	77.57	71.27	48.91	66.85	73.95	81.42	70.03
RSVQA [20]	Avg@5	75.16	67.20	40.74	42.18	65.57	57.99	67.78	46.34	34.50	67.29
	Conv@5	78.29	67.45	41.10	47.76	66.31	61.03	67.97	51.12	45.78	67.81
	Pass@5	92.51	77.95	54.86	70.64	79.20	76.71	75.86	82.34	65.43	72.14
<i>Fine-grained Grounding</i>											
DIOR-RSVG [46]	IoU@50	47.00	35.40	34.51	7.16	24.28	3.21	2.73	4.37	17.67	44.63
	IoU@70	33.32	20.84	20.76	0.93	13.35	0.43	0.20	1.29	7.21	29.37
	mIoU	45.29	35.64	33.96	12.84	25.48	8.91	6.87	7.82	20.97	40.32
VRSBench-Ref [17]	IoU@50	54.71	19.10	35.56	26.46	24.69	3.5	14.64	1.97	17.18	33.13
	IoU@70	32.40	7.58	18.74	11.95	11.83	0.63	6.33	0.36	13.77	35.40
	mIoU	48.04	21.99	34.07	27.55	25.29	8.62	15.69	5.48	4.51	18.74

4. Experiments

Experimental Design. Our experiments are designed to (1) evaluate the effectiveness of the RS-EoT paradigm and (2) provide in-depth analyses of its mechanisms. For evaluation, we conduct quantitative comparisons against SOTA models on VQA and grounding tasks (Sec. 4.1). We also compare our SocraticAgent data against traditional distillation methods (Sec. 4.2). For analysis, we provide case studies illustrating RS-EoT-7B’s iterative evidence-seeking (Sec. 4.3) and analyze attention dynamics to show its reasoning-perception cycles (Sec. 4.4). We also present the VQA-RL reward curve to validate our data strategy (Sec. 4.5). Finally, we conduct a stage-wise ablation study to verify the contribution of each component (Sec. 4.6).

Implementation details. We set a 6-round dialogue limit for SocraticAgent and synthesize 4.3K SFT samples from the datasets listed in Tab. 2. SFT training is conducted for 5 epochs with a learning rate of 3×10^{-5} using LLaMA-Factory [48]. The two-stage RL procedure is implemented with EasyR1 [49] and GRPO [27]. In Stage 1, the model is trained on DIOR-RSVG [46] and VRSBench [17]. In Stage 2, the model is trained on RS-VQA [21] and FIT-RS [22]. Both RL stages are trained for 2 epochs with a batch size of 512 and a learning rate of 10^{-6} .

Benchmark. We evaluate on *Remote Sensing General QA* (FiT-RSFG-VQA [22], FiT-RSFG-SC [22], VRSBench-VQA [17], RSVQA [20]) and *Fine-grained Grounding* (DIOR-RSVG [46], VRSBench-Ref [17]).

Metrics. For VQA, we report Avg@5, Conv@5, and Pass@5, which evaluate the average correctness, majority correctness, and any-correct correctness among 5 generated

Table 2. Statistics of the data sources used for synthesizing our RS-EoT dataset.

Data Source	Modality	Count
FIT-RS [22]	RGB	1.9K
VRSBench [17]	RGB	1.1K
DroneVehicle [29]	RGB & INF	0.2K
SARLang-1M [38]	SAR	0.2K
EarthVQA [35]	RGB	0.6K
RSVQA [20]	RGB	0.3K
Total	RGB/INF/SAR	4.3K

Table 3. SFT performance comparison of reasoning trace synthesis strategies on FIT-RSFG-VQA. Traces generated by SocraticAgent yield stronger reasoning performance than direct distillation from frontier models (Qwen3VL, Doubao, GLM-4.5V).

Method	Avg@5	Conv@5	Pass@5
SocraticAgent (ours)	64.82	67.35	85.89
Qwen3-VL-plus [33]	63.78	65.15	76.87
Doubao-seed-1-6-vision [2]	51.80	17.17	66.81
GLM-4.5V [31]	66.25	66.58	77.99

answers, respectively. We use accuracy for classification and F1 score for multi-object recognition. For grounding, we report mIoU and IoU@N (N=50, 70), the percentage of predictions with IoU > 0.5 or 0.7, respectively.

Baseline. We compare against SOTA reasoning models (e.g., WeThink [42], Vision-R1 [10], R1-OneVision [43]) built on Qwen2.5-VL-7B [1], and RS-specific models (Geo-R1 [40], VHM-RL [13]). For data comparison, we test distillation from Qwen3-VL-plus, Doubao-seed-1-6-vision, and GLM-4.5V. We exclude Gemini/GPT-5 models as their internal processes are inaccessible.

Case#1 Q: Assuming a recently landed aircraft, is there an available gate with a jet bridge for it? A: Yes



VL-Rethinker

<think>To determine if there's an available gate with a jet bridge for a recently landed aircraft, I'll consider the following: 1. Look for open gates that don't have planes parked at them. 2. Check if any of the gates have jet bridges attached. 3. Assess the overall layout to see if there are any clear spots where an aircraft could be parked with a jet bridge. From the image, it appears that all the gates currently have aircraft parked at them. **There are no visible gaps or open spaces that would indicate an available gate with a jet bridge.** Therefore, based on this analysis, there doesn't seem to be an available gate with a jet bridge for a recently landed aircraft. </think> <answer>No</answer>

RS-EoT-7B (Ours)

<think>Alright, I will reason in a self Q&A style and give the final reply. Begin with a global check to confirm this is an airport scene and that a recently landed aircraft is present, establishing the overall context before focusing on gates and jet bridges. **Is this scene an airport with visible aircraft, runways, or taxiways? Let's look at the image. Yes, this scene is an airport.** I can see multiple aircraft parked on a large paved area, which appears to be an apron or taxiway. There are also structures that look like jet bridges connected to some of the aircraft. **Global context indicates an airport with multiple aircraft on an apron and visible jet bridges.** To determine if a recently landed aircraft can connect to a jet bridge, **the key is whether any gate position is empty; if so, the aircraft can park there and use the adjacent jet bridge.** I will ask a targeted question about the presence of an empty gate position. **Is there at least one empty jet bridge gate position visible (i.e., a gate with no aircraft parked at it)? Let's look at the image. Yes, there is at least one empty jet bridge gate position visible.** In the upper central part of the image, there is a jet bridge extending from a building, but no aircraft is parked at it. **Global view confirms an airport with multiple aircraft and jet bridges. Targeted check indicates at least one empty jet bridge gate position.** Therefore, a recently landed aircraft could park at that gate and use the adjacent jet bridge. Final review finds no contradictions. </think> **Yes**

Case#2 Q: Locate the water in the image. Return the coordinates as "[x1, y1, x2, y2]".



Wethink

<think>There is no visible water body in the image. The image shows a rural area with a cluster of buildings and agricultural fields. The fields appear to be dry and possibly recently plowed, and **there are no signs of water bodies such as ponds, rivers, or lakes.** </think> <answer>There is no water in the image.</answer>

RS-EoT-7B (Ours)

<think>Alright, I will reason in a self Q&A style and give the final reply. Start with a global check for major water bodies to establish the primary water extent in the scene. **Is there a large continuous water body occupying a significant portion of the image? Let's look at the image. No, there is not a large continuous water body occupying a significant portion of the image.** There are a few small, irregularly shaped water bodies, but none are large or continuous enough to fit the description. To refine the global understanding, confirm whether any large water bodies exist at all, since the initial check suggested none. **Is there any large water body visible in the image? Let's look at the image. Yes, there is a large water body visible. It is located towards the bottom left of the image, appearing as a dark, somewhat crescent-shaped area within a green field.** This water body is large enough to be considered a significant feature in the scene. We need to confirm the exact count of major water bodies to structure the location description. **Is there exactly one distinct large water body visible in the image? Let's look at the image, yes, there is exactly one distinct large water body visible in the image.** It is located in the lower-left quadrant of the image. We have identified one distinct large water body in the lower-left quadrant. To refine the location description, confirm whether any additional water is present elsewhere in the image. **Is there any other water body visible outside the lower-left quadrant? Let's look at the image. No, there is no other water body visible outside the lower-left quadrant. The only other water bodies are located within or near the lower-left quadrant.** There is a contradiction about whether the lower-left water body is crescent-shaped or irregular. Verify the water body's shape to finalize the location description. **Is the water body in the lower-left quadrant mostly crescent-shaped? Let's look at the image. The water body in the lower-left quadrant is mostly irregular in shape, appearing to be a dark, somewhat blob-like feature within a larger green field. It does not have a distinct crescent shape.** Global and detailed observations confirm a single distinct water body in the lower-left quadrant that is irregularly shaped and lies within a green field; no other water bodies are present elsewhere. Final checks indicate no additional water features at the margins. </think> [16, 526, 293, 666]



Figure 3. Case studies comparing RS-EoT-7B with prior multimodal reasoning models on (top) Remote Sensing General QA and (bottom) Fine-grained Grounding. Unlike previous models, RS-EoT-7B follows the RS-EoT paradigm: it iteratively self-questions, gathers additional visual evidence during reasoning, and uses that evidence to verify or adjust its conclusions.

4.1. Comparison with Prior Reasoning Models

Tab. 1 compares RS-EoT-7B with recent multimodal reasoning models and two RS specific reasoning models across both remote sensing VQA and fine-grained grounding benchmarks. Except for Geo-R1 and VHM-RL, all competing models are built on Qwen2.5-VL-7B, ensuring a fair comparison focused on the effectiveness of the reasoning paradigm rather than the capacity of the base model.

On the remote sensing VQA benchmarks, RS-EoT-7B consistently achieves the best performance across all three evaluation metrics (Avg@5, Conv@5, Pass@5), indicating stronger reasoning ability and more stable answer quality. In contrast, existing multimodal reasoning models exhibit noticeable instability: their performance fluctuates significantly relative to the base model and fails to deliver consistent gains on remote sensing tasks, suggesting that their generated reasoning traces primarily reflect *pseudo reasoning* rather than genuine evidence-guided reasoning.

For fine-grained grounding tasks, RS-EoT-7B also surpasses all baselines by a large margin in IoU@50, IoU@70, and mIoU. These improvements demonstrate that the iterative evidence-seeking mechanism effectively guides the model's attention to and improves its ability to localize visual cues.

4.2. Comparison with Frontier Model Distillation

We compare our SocraticAgent against the common practice of directly distilling reasoning traces from frontier mod-

els. We sampled 2K queries from the FIT-RSFG-VQA training set and generated reasoning traces in two ways: (1) using our SocraticAgent, and (2) via direct distillation from Qwen3-VL-plus, Doubao-seed-1-6-vision, and GLM-4.5V. We then fine-tuned models on each dataset and evaluated them on FIT-RSFG-VQA, with results shown in Tab. 3.

The results show that models trained on SocraticAgent-generated traces consistently outperform those trained on directly distilled traces. This suggests that frontier models often do not expose reasoning processes aligned with remote sensing cognition. In contrast, SocraticAgent synthesizes structured, iterative, and evidence-seeking trajectories, leading to more reliable and transferable reasoning behavior in remote sensing.

4.3. Case Study

We present two qualitative examples in Fig. 3 to illustrate the RS-EoT paradigm. In the VQA example, the baseline performs only a single, coarse scene interpretation and fails to find an available jet bridge, missing contradictory visual evidence. In contrast, RS-EoT-7B performs iterative verification: it first establishes the airport context, then explicitly searches for an *unoccupied* gate, and finally identifies an available one. In the grounding example, the baseline fails to detect the small, irregular water body. RS-EoT-7B, however, uses iterative inspection guided by self-questioning: it first performs a global scan, then identifies a candidate region (lower-left), and re-examines the image to rule out

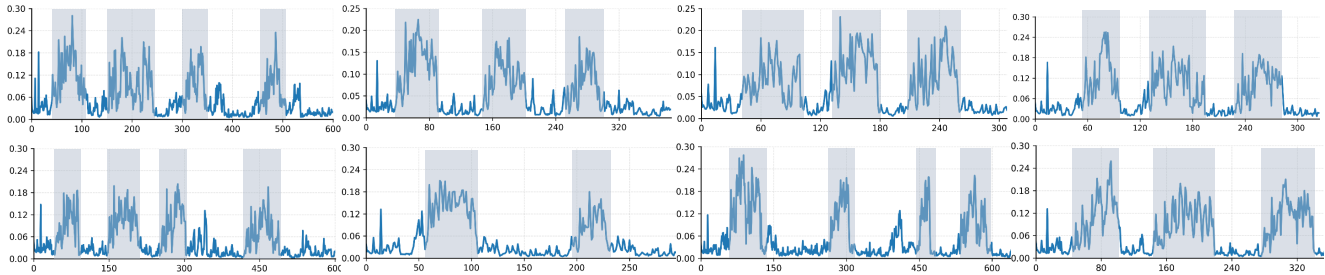


Figure 4. Token-wise attention visualization on eight randomly sampled cases. The y-axis represents the proportion of attention allocated to image tokens, and the x-axis represents the token index during the decoding step. Clear periodic patterns emerge: attention peaks on visual tokens (evidence-seeking phases) and then drops during language-based reasoning (reasoning phases). This alternating cycle reflects the iterative reasoning mechanism instilled by the RS-EoT paradigm.

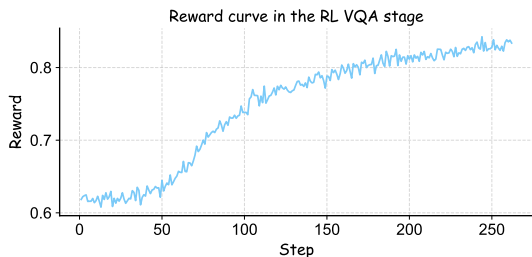


Figure 5. The reward curve for the VQA RL stage. The stable upward trend validates that our multiple-choice data reconstruction strategy provides an effective learning signal and successfully mitigates reward hacking.

other water bodies. This sequence of targeted visual checks allows the model to refine both what is present and where it is located, ultimately producing accurate coordinates supported by its grounded reasoning.

4.4. Attention Dynamics During EoT Reasoning

To understand how RS-EoT guides the model to alternate between linguistic reasoning and visual evidence seeking, we visualize the token-wise attention distribution during decoding. For each generated token, we compute the proportion of its attention allocated to image tokens (y-axis) plotted against its index in the generated sequence (x-axis).

Fig. 4 presents visualizations on eight randomly sampled test cases, all revealing a clear periodic pattern. Attention periodically peaks on visual tokens, which we interpret as *evidence-seeking phases* where the model actively retrieves new visual cues from the image. These peaks are followed by troughs where attention shifts back to language tokens, corresponding to *reasoning phases* for linguistic deduction. This alternating behavior aligns precisely with our RS-EoT paradigm, demonstrating that the model dynamically coordinates between image inspection and high-level inference, rather than merely generating text sequentially. These findings confirm that RS-EoT enables a structured, iterative reasoning process where the model repeatedly examines the image, updates its hypothesis, and advances its reasoning.

Table 4. Ablation study of training stages on VQA and Grounding and the results validate the complementary role of each stage.

Stage	VQA			Grounding		
	Avg@5	Conv@5	Pass@5	IoU@50	IoU@70	mIoU
Base	67.20	67.45	77.95	35.40	20.84	35.64
+SFT	70.73	74.05	91.96	8.81	2.19	13.95
+RL-IoU	69.51	72.01	90.63	48.41	33.51	45.57
+RL-VQA	75.16	78.29	92.51	48.23	33.27	45.52

4.5. VQA-RL Training Stability Analysis

Fig. 5 illustrates the reward curve during the VQA RL stage (Stage#2). We observe a smooth and consistent upward trajectory, with the reward steadily increasing from an initial value of approximately 0.62 and converging around 0.84. This stable progression provides strong evidence for the effectiveness of our multiple-choice data reconstruction strategy. It demonstrates that our method, combined with the tailored graded reward function, successfully mitigates reward hacking and provides a stable, effective learning signal, enabling the model to learn from simple RS VQA datasets without training collapse.

4.6. Stage-wise Training Analysis

We conduct a stage-wise ablation to analyze the contribution of each training step, as shown in Tab. 4. Starting from the Base model, SFT with RS-EoT trajectories substantially improves VQA accuracy but causes a significant drop in grounding ability. The subsequent RL-IoU stage effectively restores and dramatically enhances grounding performance, confirming that explicit spatial feedback is crucial for localization. Finally, the RL-VQA stage further improves VQA reasoning while successfully maintaining the strong grounding performance. These results highlight the complementary role of each stage: SFT injects the reasoning pattern, RL-IoU enhances the visual evidence-seeking capability, and RL-VQA allows the model to be applied to broader remote sensing scenarios.

5. Conclusion

In this work, we introduce RS-EoT, an iterative evidence-seeking paradigm for remote sensing understanding. RS-EoT structures reasoning as an alternating loop of linguistic deduction and targeted visual evidence seeking. We instill this paradigm using an SFT and progressive RL (Grounding+VQA) pipeline. Experiments show our approach surpasses SOTA baselines in reasoning robustness and grounding accuracy. Analyses confirm the model internalizes this iterative pattern, validating structured reasoning for trustworthy geospatial AI.

References

- [1] Shuai Bai, Keqin Chen, Xuejing Liu, Jialin Wang, Wenbin Ge, Sibao Song, Kai Dang, Peng Wang, Shijie Wang, Jun Tang, et al. Qwen2. 5-vl technical report. *arXiv preprint arXiv:2502.13923*, 2025. 6
- [2] ByteDance / Volcengine. Seed 1.6 — doubao (seed) 1.6. Online, 2025. 1, 4, 6
- [3] Hardy Chen, Haoqin Tu, Fali Wang, Hui Liu, Xianfeng Tang, Xinya Du, Yuyin Zhou, and Cihang Xie. Sft or rl? an early investigation into training rl-like reasoning large vision-language models. *arXiv preprint arXiv:2504.11468*, 2025. 2, 3, 6
- [4] Wenhui Chen, Xueguang Ma, Xinyi Wang, and William W. Cohen. Program of thoughts prompting: Disentangling computation from reasoning for numerical reasoning tasks. *Transactions on Machine Learning Research*, 2023. 3
- [5] Gheorghe Comanici, Eric Bieber, Mike Schaeckermann, Ice Pasapat, Noveen Sachdeva, Inderjit Dhillon, Marcel Blisstein, Ori Ram, Dan Zhang, Evan Rosen, et al. Gemini 2.5: Pushing the frontier with advanced reasoning, multimodality, long context, and next generation agentic capabilities. *arXiv preprint arXiv:2507.06261*, 2025. 4
- [6] Chenrui Fan, Ming Li, Lichao Sun, and Tianyi Zhou. Missing premise exacerbates overthinking: Are reasoning models losing critical thinking skill? *arXiv preprint arXiv:2504.06514*, 2025. 2
- [7] Gongfan Fang, Xinyin Ma, and Xinchao Wang. Thinkless: Llm learns when to think. *Advances in neural information processing systems*, 2025. 2
- [8] Daya Guo, Dejian Yang, Haowei Zhang, Junxiao Song, Peiyi Wang, Qihao Zhu, Runxin Xu, Ruoyu Zhang, Shirong Ma, Xiao Bi, et al. Deepseek-r1 incentivizes reasoning in llms through reinforcement learning. *Nature*, 645(8081):633–638, 2025. 1, 2, 3
- [9] Xin Guo, Jiangwei Lao, Bo Dang, Yingying Zhang, Lei Yu, Lixiang Ru, Liheng Zhong, Ziyuan Huang, Kang Wu, Dingxiang Hu, Huimei He, Jian Wang, Jingdong Chen, Ming Yang, Yongjun Zhang, and Yansheng Li. Skysense: A multimodal remote sensing foundation model towards universal interpretation for earth observation imagery. In *Proceedings of the IEEE/CVF Conference on Computer Vision and Pattern Recognition (CVPR)*, pages 27672–27683, 2024. 2
- [10] Wenxuan Huang, Bohan Jia, Zijie Zhai, Shaosheng Cao, Zheyu Ye, Fei Zhao, Zhe Xu, Yao Hu, and Shaohui Lin. Vision-r1: Incentivizing reasoning capability in multimodal large language models. *arXiv preprint arXiv:2503.06749*, 2025. 2, 3, 6
- [11] Ziyue Huang, Hongxi Yan, Qiqi Zhan, Shuai Yang, Mingming Zhang, Chenkai Zhang, YiMing Lei, Zeming Liu, Qingjie Liu, and Yunhong Wang. A survey on remote sensing foundation models: From vision to multimodality. *arXiv preprint arXiv:2503.22081*, 2025. 2
- [12] Aaron Jaech, Adam Kalai, Adam Lerer, Adam Richardson, Ahmed El-Kishky, Aiden Low, Alec Helyar, Aleksander Madry, Alex Beutel, Alex Carney, et al. Openai o1 system card. *arXiv preprint arXiv:2412.16720*, 2024. 3
- [13] Aybora Köksal and A Aydın Alatan. Few-shot vision-language reasoning for satellite imagery via verifiable rewards. In *Proceedings of the IEEE/CVF International Conference on Computer Vision*, pages 6901–6910, 2025. 3, 6
- [14] Kartik Kuckreja, Muhammad Sohail Danish, Muzammal Naseer, Abhijit Das, Salman Khan, and Fahad Shahbaz Khan. Geochat: Grounded large vision-language model for remote sensing. In *Proceedings of the IEEE/CVF Conference on Computer Vision and Pattern Recognition*, pages 27831–27840, 2024. 2
- [15] Haodong Li, Xiaofeng Zhang, and Haicheng Qu. Ddfav: Remote sensing large vision language models dataset and evaluation benchmark. *Remote Sensing*, 17(4):719, 2025. 2
- [16] Kun Li, George Vosselman, and Michael Ying Yang. Hrvqa: A visual question answering benchmark for high-resolution aerial images. *ISPRS Journal of Photogrammetry and Remote Sensing*, 214:65–81, 2024. 5
- [17] Xiang Li, Jian Ding, and Mohamed Elhoseiny. Vrsbench: A versatile vision-language benchmark dataset for remote sensing image understanding. *Advances in Neural Information Processing Systems*, 37:3229–3242, 2024. 6
- [18] Xiang Li, Congcong Wen, Yuan Hu, Zhenghang Yuan, and Xiao Xiang Zhu. Vision-language models in remote sensing: Current progress and future trends. *IEEE Geoscience and Remote Sensing Magazine*, 12(2):32–66, 2024. 2
- [19] Chenyang Liu, Jiafan Zhang, Keyan Chen, Man Wang, Zhengxia Zou, and Zhenwei Shi. Remote sensing spatiotemporal vision-language models: A comprehensive survey. *IEEE Geoscience and Remote Sensing Magazine*, 2025. 2
- [20] Sylvain Lobry, Diego Marcos, Jesse Murray, and Devis Tuia. Rsvqa: Visual question answering for remote sensing data. *IEEE Transactions on Geoscience and Remote Sensing*, 58(12):8555–8566, 2020. 6
- [21] Sylvain Lobry, Begüm Demir, and Devis Tuia. Rsvqa meets bigearthnet: A new, large-scale, visual question answering dataset for remote sensing. In *2021 IEEE International Geoscience and Remote Sensing Symposium IGARSS*, pages 1218–1221, 2021. 5, 6
- [22] Junwei Luo, Zhen Pang, Yongjun Zhang, Tingzhu Wang, Linlin Wang, Bo Dang, Jiangwei Lao, Jian Wang, Jingdong Chen, Yihua Tan, and Yansheng Li. Skysensegpt: A fine-grained instruction tuning dataset and model for remote sensing vision-language understanding, 2024. 5, 6
- [23] Fanqing Meng, Lingxiao Du, Zongkai Liu, Zhixiang Zhou, Quanfeng Lu, Daocheng Fu, Tiancheng Han, Botian Shi,

- Wenhai Wang, Junjun He, Kaipeng Zhang, Ping Luo, Yu Qiao, Qiaosheng Zhang, and Wenqi Shao. Mm-eureka: Exploring the frontiers of multimodal reasoning with rule-based reinforcement learning, 2025. 2, 3, 6
- [24] OpenAI. Gpt-5 system card. <https://cdn.openai.com/gpt-5-system-card.pdf>, 2025. 4
- [25] Pranav Saxena, Nishant Raghuvanshi, and Neena Goveas. Uav-vln: End-to-end vision language guided navigation for uavs. In *2025 European Conference on Mobile Robots (ECMR)*, page 1–6. IEEE, 2025. 2
- [26] John Schulman, Filip Wolski, Prafulla Dhariwal, Alec Radford, and Oleg Klimov. Proximal policy optimization algorithms. *arXiv preprint arXiv:1707.06347*, 2017. 3
- [27] Zhihong Shao, Peiyi Wang, Qihao Zhu, Runxin Xu, Junxiao Song, Mingchuan Zhang, Y. K. Li, Y. Wu, and Daya Guo. Deepseekmath: Pushing the limits of mathematical reasoning in open language models, 2024. 3, 6
- [28] Chuming Shen, Wei Wei, Xiaoye Qu, and Yu Cheng. Satorir1: Incentivizing multimodal reasoning with spatial grounding and verifiable rewards, 2025. 2
- [29] Yiming Sun, Bing Cao, Pengfei Zhu, and Qinghua Hu. Drone-based rgb-infrared cross-modality vehicle detection via uncertainty-aware learning. *IEEE Transactions on Circuits and Systems for Video Technology*, pages 1–1, 2022. 6
- [30] Lijie Tao, Haokui Zhang, Haizhao Jing, Yu Liu, Dawei Yan, Guoting Wei, and Xizhe Xue. Advancements in vision-language models for remote sensing: Datasets, capabilities, and enhancement techniques. *Remote Sensing*, 17(1):162, 2025. 2
- [31] GLM-V Team. Glm-4.5v and glm-4.1v-thinking: Towards versatile multimodal reasoning with scalable reinforcement learning, 2025. 6
- [32] Kimi Team, Angang Du, Bofei Gao, BOWEI XING, Changjiu Jiang, Cheng Chen, Cheng Li, Chenjun Xiao, Chenzhuang Du, Chonghua Liao, et al. Kimi k1.5: Scaling reinforcement learning with llms. *arXiv preprint arXiv:2501.12599*, 2025. 2
- [33] Qwen Team. Qwen3-vl: Sharper vision, deeper thought, broader action. *Qwen Blog*. Accessed, pages 10–04, 2025. 6
- [34] Haozhe Wang, Chao Qu, Zuming Huang, Wei Chu, Fangzhen Lin, and Wenhui Chen. Vl-rethinker: Incentivizing self-reflection of vision-language models with reinforcement learning. *arXiv preprint arXiv:2504.08837*, 2025. 2, 3, 6
- [35] Junjue Wang, Zhuo Zheng, Zihang Chen, Ailong Ma, and Yanfei Zhong. Earthvqa: Towards queryable earth via relational reasoning-based remote sensing visual question answering. *Proceedings of the AAAI Conference on Artificial Intelligence*, 38(6):5481–5489, 2024. 6
- [36] Peijin Wang, Huiyang Hu, Boyuan Tong, Ziqi Zhang, Fanglong Yao, Yingchao Feng, Zining Zhu, Hao Chang, Wenhui Diao, Qixiang Ye, and Xian Sun. Ringmogpt: A unified remote sensing foundation model for vision, language, and grounded tasks. *IEEE Transactions on Geoscience and Remote Sensing*, 63:1–20, 2025. 2
- [37] Jason Wei, Xuezhi Wang, Dale Schuurmans, Maarten Bosma, Fei Xia, Ed Chi, Quoc V Le, Denny Zhou, et al. Chain-of-thought prompting elicits reasoning in large language models. *Advances in neural information processing systems*, 35:24824–24837, 2022. 3
- [38] Yimin Wei, Aoran Xiao, Yexian Ren, Yuting Zhu, Hongruixuan Chen, Junshi Xia, and Naoto Yokoya. Sarlang-1m: A benchmark for vision-language modeling in sar image understanding, 2025. 6
- [39] Liang Wen, Yunke Cai, Fenrui Xiao, Xin He, Qi An, Zhenyu Duan, Yimin Du, Junchen Liu, Tanglifu Tanglifu, Xiaowei Lv, Haosheng Zou, Yongchao Deng, Shousheng Jia, and Xi-angzheng Zhang. Light-r1: Curriculum SFT, DPO and RL for long COT from scratch and beyond. In *Proceedings of the 63rd Annual Meeting of the Association for Computational Linguistics (Volume 6: Industry Track)*, pages 318–327, Vienna, Austria, 2025. Association for Computational Linguistics. 2, 3
- [40] Chenhui Xu, Fuxun Yu, Michael J. Bianco, Jacob Kovarskiy, Raphael Tang, Qi Zhang, Zirui Xu, Will LeVine, Brandon Dubbs, Heming Liao, Cassandra Burgess, Suvam Bag, Jay Patravali, Rupanjali Kukal, Mikael Figueroa, Rishi Madhok, Nikolaos Karianakis, and Jinjun Xiong. Geo-r1: Unlocking vlm geospatial reasoning with cross-view reinforcement learning, 2025. 3, 6
- [41] An Yang, Anfeng Li, Baosong Yang, Beichen Zhang, Binyuan Hui, Bo Zheng, Bowen Yu, Chang Gao, Chengen Huang, Chenxu Lv, et al. Qwen3 technical report. *arXiv preprint arXiv:2505.09388*, 2025. 1
- [42] Jie Yang, Feipeng Ma, Zitian Wang, Dacheng Yin, Kang Rong, Fengyun Rao, and Ruimao Zhang. Wethink: Toward general-purpose vision-language reasoning via reinforcement learning, 2025. 2, 3, 6
- [43] Yi Yang, Xiaoxuan He, Hongkun Pan, Xiyan Jiang, Yan Deng, Xingtao Yang, Haoyu Lu, Dacheng Yin, Fengyun Rao, Minfeng Zhu, Bo Zhang, and Wei Chen. R1-onevision: Advancing generalized multimodal reasoning through cross-modal formalization. *arXiv preprint arXiv:2503.10615*, 2025. 2, 3, 6
- [44] Qiyang Yu, Zheng Zhang, Ruofei Zhu, Yufeng Yuan, Xiaochen Zuo, Yu Yue, Weinan Dai, Tiantian Fan, Gaohong Liu, Lingjun Liu, Xin Liu, Haibin Lin, Zhiqi Lin, Bole Ma, Guangming Sheng, Yuxuan Tong, Chi Zhang, Mofan Zhang, Wang Zhang, Hang Zhu, Jinhua Zhu, Jiaye Chen, Jiangjie Chen, Chengyi Wang, Hongli Yu, Yuxuan Song, Xi-angpeng Wei, Hao Zhou, Jingjing Liu, Wei-Ying Ma, Ya-Qin Zhang, Lin Yan, Mu Qiao, Yonghui Wu, and Mingxuan Wang. Dapo: An open-source llm reinforcement learning system at scale, 2025. 3
- [45] Ruifeng Yuan, Chenghao Xiao, Sicong Leng, Jianyu Wang, Long Li, Weiwen Xu, Hou Pong Chan, Deli Zhao, Tingyang Xu, Zhongyu Wei, et al. Vl-cogito: Progressive curriculum reinforcement learning for advanced multimodal reasoning. *arXiv preprint arXiv:2507.22607*, 2025. 2
- [46] Yang Zhan, Zhitong Xiong, and Yuan Yuan. Rsvg: Exploring data and models for visual grounding on remote sensing data. *IEEE Transactions on Geoscience and Remote Sensing*, 61: 1–13, 2023. 6
- [47] Yuhang Zhang, Haosheng Yu, Jiaping Xiao, and Mir Fer-

oskhan. Grounded vision-language navigation for uavs with open-vocabulary goal understanding, 2025. 2

- [48] Yaowei Zheng, Richong Zhang, Junhao Zhang, Yanhan Ye, Zheyang Luo, Zhangchi Feng, and Yongqiang Ma. Llamafactory: Unified efficient fine-tuning of 100+ language models. In *Proceedings of the 62nd Annual Meeting of the Association for Computational Linguistics (Volume 3: System Demonstrations)*, Bangkok, Thailand, 2024. Association for Computational Linguistics. 6
- [49] Yaowei Zheng, Junting Lu, Shenzhi Wang, Zhangchi Feng, Dongdong Kuang, and Yuwen Xiong. Easyrl: An efficient, scalable, multi-modality rl training framework. <https://github.com/hiyouga/EasyRL>, 2025. 6
- [50] Denny Zhou, Nathanael Schärli, Le Hou, Jason Wei, Nathan Scales, Xuezhi Wang, Dale Schuurmans, Claire Cui, Olivier Bousquet, Quoc Le, and Ed Chi. Least-to-most prompting enables complex reasoning in large language models, 2023. 3

Asking like Socrates: Socrates helps VLMs understand remote sensing images

Supplementary Material

6. System Prompts Details

In this section, we provide the exact system prompts used in our SocraticAgent framework to synthesize the RS-EoT-4K dataset. As described in the main paper, SocraticAgent operates as a self-play multi-agent system consisting of three distinct roles: the **Reasoner**, the **Perceiver**, and the **Verifier**.

- **The Reasoner** (Fig. 6) serves as the cognitive core. It is a text-only agent designed to simulate the human “coarse-to-fine” visual interpretation process. By following a *Plan–Integrate–Decide* paradigm, it decomposes complex queries into atomic visual questions, iteratively gathering evidence before concluding.
- **The Perceiver** (Fig. 7) acts as the visual interface. To enforce explicit and detailed reasoning from the Reasoner, we employ a self-play prompting mechanism where the Perceiver is instructed to collaborate with a “weak-reasoning” partner. Its role is to provide accurate, descriptive visual observations in a “natural inner monologue” style without performing high-level logical reasoning.
- **The Verifier** (Fig. 8) functions as the quality control gatekeeper. It compares the final answer generated by the Reasoner against the ground truth to filter out incorrect or hallucinated reasoning traces during the data synthesis phase.

The complete prompts for these agents are presented in Fig. 6, Fig. 7, and Fig. 8, respectively.

7. SFT Training Settings

We perform SFT on the base model Qwen2.5-VL-7B-Instruct using the RS-EoT-4K dataset. The training is implemented based on the LLaMA-Factory framework. We train the model for 5 epochs with a learning rate of 3×10^{-5} , using the AdamW optimizer and a cosine learning rate scheduler. The global batch size is set to 64, and the maximum sequence length is limited to 4096 tokens to accommodate the detailed reasoning traces. The entire training process was executed on 4 A100 GPUs and required approximately 40 minutes to complete.

A empirical finding in our experiments concerns the use of system prompts. We observed that including explicit reasoning triggers in the system prompt (e.g., instructions like “Please reason step-by-step”) during training caused the model to develop a strong dependency on these specific triggers. Consequently, the model often failed to initiate reasoning or exhibited abnormal behaviors when such prompts were absent during inference. To address this and ensure robust, spontaneous reasoning capabilities, we exclude all

reasoning-specific instructions from the system prompt during SFT and RL. Instead, we hard-code the start-of-thought token `<think>` directly into the assistant’s response field within the chat template. This design forces the model to automatically enter the reasoning mode immediately upon generation, ensuring stable output trajectories without relying on specific user or system prompts.

8. RL Training Settings

All reinforcement learning experiments are conducted using the EasyR1 framework, which provides a production-ready implementation of GRPO with KL regularization. We fix the KL coefficient to $\beta = 1.0 \times 10^{-2}$. For each input, the model generates 4 rollout samples using sampling temperature 1.0, with a maximum response length of 4096 tokens.

Policy optimization is performed with the AdamW optimizer, using a learning rate of 1.0×10^{-6} , weight decay of 1.0×10^{-2} , and a linear warm-up over the first 3 We apply gradient clipping with a threshold of 1.0. All models are trained in `bf16` precision under full-sharded data parallelism (FSDP) with gradient checkpointing enabled.

For both RL-Grounding and RL-VQA, we use a global batch size of 512 (covering rollout, training, and validation batches) and train for 240 steps. Experiments are run on a single node equipped with 8 A100 GPUs. The RL-VQA stage requires approximately 2.3 days to complete, while the RL-Grounding stage takes about 2.5 days.

9. RL Reward Function

9.1. Grounding Reward

For the grounding task, the model is required to output a bounding box in the form $[x1, y1, x2, y2]$ after a complete `<think></think>` block. Our reward contains two components: an IoU-based accuracy term and a lightweight format term.

Format reward. For the grounding task, we apply a lightweight *format reward* to encourage the model to produce both a well-formed reasoning block and a structured bounding-box output. We evaluate two binary indicators: (i) whether the response contains a complete, matched `<think></think>` block, and (ii) whether a valid four-number bounding-box list of the form $[x1, y1, x2, y2]$ appears after the closing `</think>` tag. We denote these indicators as s_{think} and s_{bbox} , respectively. The format reward is then defined as

$$r_{\text{fmt}} = \frac{s_{\text{think}} + s_{\text{bbox}}}{2},$$

System Prompt for the Reasoner

You are a reasoning model that follows a **Plan–Integrate–Decide** paradigm, collaborating with a **weak-perception visual model** to complete **general remote sensing tasks** (such as classification/attribute recognition, localization/counting, relation/change detection, and VQA). The perception model can only answer **very simple, atomic visual facts** and cannot perform reasoning. Therefore, you must decompose the perception process into a **coarse-to-fine sequence of steps**, simulating how humans visually interpret remote sensing imagery.

[Coarse-to-Fine Perception Chain]

1) Global Observation Stage (Overall Understanding):

- Begin with a **broad, holistic examination** of the entire image, forming an initial impression of its overall layout — main land-cover types, spatial organization, scene functionality, distribution of major objects, and possible visual interferences (e.g., shadows, fog, noise, or occlusion).
- While questions at this stage should remain **broad, general, and high-level**, they must be **context-aware** — i.e., lightly tailored to the task/query so they inform later reasoning for this specific problem.

2) Focused and Detailed Observation Stage (Targeted Analysis):

- After forming a general understanding of the scene, use the task objective (query) and global observations to **focus attention** on potentially relevant local regions or objects.
- Naturally shift attention from overall impressions to specific, task-relevant areas, similar to how humans visually focus.
- Ask more detailed and targeted questions, typically focusing on:
 - Local details (shape, texture, boundaries, orientation, color features, etc.);
 - Relationships and differences (changes, similarities, transitions between regions, etc.);
 - Task-critical elements (e.g., presence, quantity, or arrangement of specific targets).

3) Integration and Verification Stage:

- Integrate the facts collected from the global and detailed observation stages into a consistent intermediate conclusion.
- If contradictions or uncertainties remain, ask verification questions.
- Ensure that the reasoning covers all key regions and that the logic is consistent.

4) Final Review and Confirmation Stage:

- Before giving the final answer, perform a quick overall review of the image to confirm that no small anomalies, marginal areas, or potential clues have been overlooked.
- Check whether the final answer meets the query’s requirements regarding format, length, and structure.
- The final answer must only output the direct answer to the query itself, such as “Yes/No”, a specific number, or a concise conclusion. Do not include any explanations, reasoning, or additional commentary.
- If necessary, ask one final targeted question for confirmation.

[Questioning and Iteration Constraints]

- **Never** forward the user’s original query directly to the perception model; each question must concern **only one atomic visual fact**.
- Each new question should provide **maximum information gain** and **must not repeat** previous questions (avoid paraphrasing).
- You have $\{\text{MAX_LOOP}-1\}$ questioning rounds available: the early rounds focus on global perception, the middle rounds gather key evidence, and the final rounds perform verification questioning.

[Output Format (Strict Requirements)]

- If further questioning is needed:

Start with `<thinking>...</thinking>` (briefly explain the reasoning and purpose of the next question), then output **only one** `<question>...</question>`.

- If ready to give the final answer:

Start with `<thinking>...</thinking>` (summarize key evidence and note that final checks have been completed), then output `\{FINAL_PREFIX_EN\} ...`

- Each round must **begin** with `<thinking>...</thinking>` and be followed by **exactly one** of the two options: `<question>...</question>` or `\{FINAL_PREFIX_EN\} ...`. No other content is allowed.

- Inside `<thinking>`, do **not** mention external entities such as “the perception model,” “user,” or “conversation.”

- Use **English** for internal reasoning and questioning, but ensure that the **final answer matches the input query’s language**.

Figure 6. The system prompt for the Reasoner in SocraticAgent.

IoU accuracy. We first normalize the response and verify that a well-formed reasoning block (i.e., a matched pair `<think>...</think>`) exists. Only the text appearing *after* the closing tag `</think>` is used for prediction parsing. From this tail segment, we extract the first valid four-number list $[x_1, y_1, x_2, y_2]$; if no valid list is found, the prediction is treated as invalid. The accuracy score is then computed using the IoU between the predicted and ground-truth boxes directly in the original pixel coordi-

nate system:

$$r_{\text{acc}} = \begin{cases} \text{IoU}(\text{bbox}_{\text{pred}}, \text{bbox}_{\text{gt}}), & \text{if a valid box is parsed,} \\ 0, & \text{otherwise.} \end{cases}$$

Overall reward. The final grounding reward combines IoU accuracy and the format term:

$$r_{\text{overall}} = (1 - \lambda) r_{\text{acc}} + \lambda r_{\text{fmt}},$$

System Prompt for the Perceiver

You are an image interpretation expert collaborating with a **reasoning model that has very weak logical ability**. Together, through multi-turn dialogue, you will complete **general remote sensing tasks** (classification/attribute, localization/counting, relation/change analysis, VQA, etc.). The reasoning model can **only understand the textual descriptions** of your perception results — it **cannot see the image directly**. Therefore, you must respond to each of its questions about the image **accurately and completely**, without adding any information that is irrelevant to the question. Your tone should resemble a **natural inner monologue** of a person carefully observing an image. Always begin your response with: "Let's look at the image," and then continue with your detailed observation.

Figure 7. The system prompt for the Perceiver in SocraticAgent.

System Prompt for the Verifier

You are a **strict answer evaluator**. Given a Query, Answer, and GT, output only:
1) "ACCEPT"
2) "REJECT: <brief reason>"

Figure 8. The system prompt for the Verifier in SocraticAgent.

where we use $\lambda = 0.1$ in all experiments. Each sample is scored independently, and we log r_{overall} , IoU, r_{acc} , and r_{fmt} during training.

9.2. Multiple-Choice VQA Reward

For the multiple-choice VQA task, the model predicts a subset of option letters (e.g., A, C, D) after completing the `<think></think>` reasoning block. Only the text following the last `</think>` tag is considered for answer extraction. We first identify the last line in this tail that contains independent letter tokens; if none are found, we treat the prediction as invalid.

Given the ground-truth correct set $G \subseteq \mathcal{A}$ and the model's predicted set $P \subseteq \mathcal{A}$, where \mathcal{A} is the set of all allowed options, we compute a symmetric, option-level accuracy score. Each option contributes equally: selecting a correct option and correctly rejecting an incorrect option both receive positive credit, while selecting an incorrect option or failing to select a correct one is penalized. The accuracy reward is therefore:

$$r_{\text{acc}} = 1 - \frac{1}{|\mathcal{A}|} \sum_{a \in \mathcal{A}} |\mathbf{1}\{a \in G\} - \mathbf{1}\{a \in P\}|.$$

If the model outputs any letter not contained in \mathcal{A} , we apply a hard-zero accuracy (i.e., $r_{\text{acc}} = 0$), matching our implementation.

Format reward. The VQA setting uses the same lightweight format reward as the grounding task. Because empty outputs are allowed and interpreted as selecting no options, the format reward does not require the predicted letters to appear after the `</think>` tag. Instead, we

simply check whether the model produces a complete and matched `<think></think>` reasoning block. If the block is present, the model earns a format score of 1; otherwise, the score is 0.

Overall reward. The final VQA reward is a convex combination of accuracy and format:

$$r_{\text{overall}} = (1 - \lambda) r_{\text{acc}} + \lambda r_{\text{fmt}},$$

with $\lambda = 0.1$ throughout all experiments.

This reward design provides a graded, stable learning signal across all options without relying on task-specific heuristics, while the matched `<think></think>` constraint ensures structured reasoning outputs.

10. RL Training Dynamics Curves

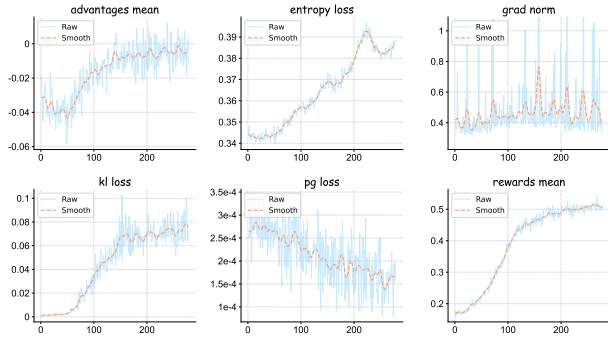
Figure 9 visualizes the evolution of key optimization statistics during the two RL stages in our pipeline: RL-Grounding and RL-VQA. The top block corresponds to the RL Grounding stage and the bottom block to the RL-VQA stage; in both cases we plot the same set of metrics, including mean advantage, actor gradient norm, entropy loss, KL loss, policy gradient loss, and average reward. For each quantity, we plot both the raw measurements and their Gaussian-smoothed trends, providing a compact view of how the GRPO optimization behaves over the training steps in both stages.

11. Difference Between Multiple-Choice VQA and Standard VQA

To assess the effectiveness of our proposed multiple-choice reformulation of VQA, we additionally perform an ablation study using the original dataset and model settings, but applying reinforcement learning directly on the *standard* free-form VQA answers. This experiment allows us to isolate and compare the impact of our multiple-choice VQA design against the conventional VQA supervision.

We first evaluate the final model performance on the RSVQA. As presented in Table 5, our multiple-choice reconstruction strategy achieves consistently superior results

RL-Grounding Training Dynamics



RL-VQA Training Dynamics

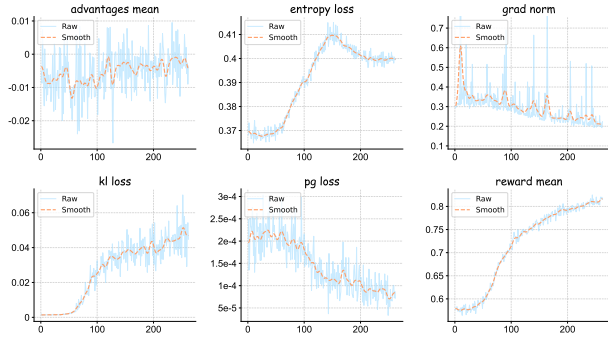


Figure 9. RL training dynamics for our two-stage pipeline. Top: RL-Grounding stage; bottom: RL-VQA stage. Each panel reports the evolution of a different statistic (advantages mean, entropy loss, gradient norm, KL loss, policy gradient loss, and rewards mean), with light curves showing raw values and dashed curves showing Gaussian-smoothed trends over training steps.

across all metrics compared to the standard free-form supervision. To understand the underlying cause of this performance gap, we visualize the training stability in Figure 10. When trained with standard free-form VQA answers, the model exhibits slow reward improvement and frequent large-magnitude oscillations during GRPO optimization. This indicates that the original VQA supervision produces an unstable and inefficient reward signal for RL, making it difficult for the model to learn consistent behaviors. In contrast, our multiple-choice VQA reformulation leads to a much smoother and steadily increasing reward curve under the *same* RL setup. This demonstrates that transforming VQA into a structured multi-option prediction task greatly stabilizes the reward landscape and improves training efficiency.

Overall, the ablation confirms that the multiple-choice VQA formulation provides a more reliable and effective RL objective compared to standard VQA, and is essential for

Table 5. Ablation study on VQA data reconstruction strategies on the RSVQA. We compare our proposed Multiple-Choice VQA reconstruction against the Standard VQA (Free-form) supervision. Our method achieves consistently superior performance across all metrics.

Method	Avg@5	Conv@5	Pass@5
Standard VQA (Free-form)	74.73	76.86	90.91
Ours (Multiple-Choice)	75.16	78.29	92.51

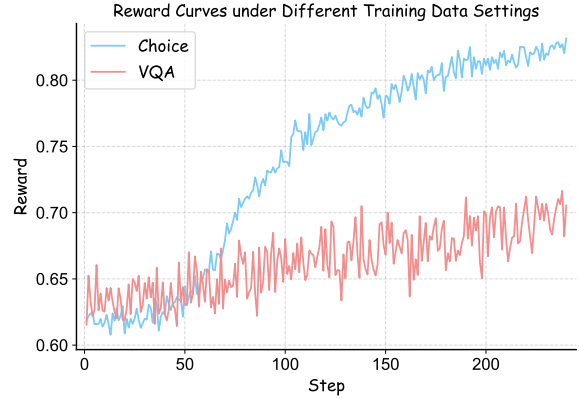


Figure 10. Ablation comparing reinforcement learning on the original free-form VQA answers (red) versus our reconstructed multiple-choice VQA reconstruction (blue). Standard VQA produces unstable and oscillatory training dynamics, while the multiple-choice approach yields smooth and efficient reward improvement.

achieving stable reinforcement learning in our setting.

12. Case Study

We provide additional qualitative examples to further demonstrate the effectiveness of RS-EoT-7B in complex remote sensing reasoning scenarios. Specifically, we present extended case studies covering both Remote Sensing General VQA tasks (Fig. 11, Fig. 12, and Fig. 13) and Fine-grained Grounding tasks (Fig. 14 and Fig. 15). These visualizations illustrate how the model employs the iterative evidence-seeking paradigm to achieve robust reasoning and precise localization across diverse queries.

Q: What is the runway designation shown in the image?



Alright, I will reason in a self Q&A style and give the final reply. Start with a global check to confirm the scene contains runway-like infrastructure before focusing on specific markings. Is there a long, wide, straight paved strip visible in the image? Let's look at the image. Yes, there is a prominent long, wide, straight paved strip visible in the image. It is a gray surface with white and yellow markings, running diagonally across the image from the top-center towards the bottom-left. Focus on the strip's markings to identify the runway designation associated with the visible numbers. Are there large white runway numbers visible on the paved strip? Let's look at the image, yes, there are large white runway numbers visible on the paved strip. Specifically, the number "36" is clearly visible, with an additional "L" next to it. Global view confirmed a long, wide runway; detailed check verified large white runway numbers "36" with an additional "L." No inconsistencies detected; this is a standard runway designation. Final review complete.</think> 36L

Q: Are there any vehicles about to enter the ramp?



Alright, I will reason in a self Q&A style and give the final reply. Start with a global check to confirm the presence of a ramp-like road connection, which is essential before assessing vehicles entering it. Is there a distinct road ramp connection visible, such as an on-ramp or off-ramp, merging into the main highway? Let's look at the image. Yes, there is a distinct road ramp connection visible. A curved road, located in the bottom right portion of the image, merges into the main highway. This ramp is clearly separated from the main highway by a grassy area, and it features white road markings, including chevron-like shapes at its entrance, indicating it's a ramp connection. With the ramp connection confirmed, focus on whether any vehicles are positioned on it, which directly addresses the query about vehicles entering the ramp. Are there any vehicles visible on the ramp road near the ramp entrance? Let's look at the image. Yes, there is one vehicle visible on the ramp road near the ramp entrance. It is a white vehicle, positioned on the lane that curves to the right in the bottom right portion of the image. The scene includes a distinct ramp connection, and one white vehicle is visible on the ramp near the entrance, which qualifies as a vehicle about to enter the ramp. No contradictions found upon review.</think> Yes

Q: If I start from the yellow construction site in the lower-left corner and walk along the road to the parking lot in the upper-right corner, how many intersections will I pass through?



Alright, I will reason in a self Q&A style and give the final reply. Start with a global check to confirm the presence and location of the target yellow construction site to anchor the walk route. Is there a yellow construction site located in the lower-left corner of the image? Let's look at the image. Yes, there is an area that appears to be a yellow construction site located in the lower-left corner of the image. It's a large, irregularly shaped area with a light brown, earthy tone, distinct from the surrounding grey roads and building rooftops. We have confirmed the starting point (yellow construction site) is in the lower-left and the destination (parking lot) is in the upper-right. Next, to mentally map the walk route, we should verify whether there is a major road running vertically near the center, which would align with a likely walking path toward the upper-right corner. Is there a prominent vertical road running near the center of the image? Let's look at the image, yes, there is a prominent vertical road running near the center of the image. It's a wide, dark gray paved road that extends from the top edge of the image all the way down to the bottom edge, passing through the

middle section. We have identified the starting point (yellow construction site, lower-left) and the general destination (parking lot, upper-right). A prominent vertical road runs through the center, so the most direct path toward the upper-right will cross this central road. To determine the exact count, we need to know how many times the central road is crossed along the way. How many times does the prominent vertical road intersect other roads along the route from the yellow construction site to the parking lot in the upper-right corner? Let's look at the image. I need to identify the prominent vertical road, locate the yellow construction site, and a parking lot in the upper-right corner. Then I will count how many times the prominent vertical road intersects other roads along that route.1. ****Locating the Prominent Vertical Road****: The most prominent vertical road is a wide, dark gray road that runs from the top of the image down towards the bottom, passing through the center.2. ****Identifying the Yellow Construction Site****: The yellow construction site is located in the bottom-left corner of the image, characterized by a large, irregular area of bare earth with some yellow markings.3. ****Identifying a Parking Lot in the Upper-Right Corner****: There is a large parking lot with many cars in the upper-right portion of the image, located near several buildings with light-colored roofs. Now, I will mentally trace the route from the yellow construction site to the upper-right parking lot along the prominent vertical road and count the intersections. Starting from the bottom-left corner (yellow construction site), the route goes straight up along the prominent vertical road. Along this path, the first road encountered and crossed above the main vertical road is a horizontal road that runs roughly from the left edge to the right edge, intersecting the prominent vertical road in the middle-left area of the image. This is the first intersection. After crossing this first horizontal road, the route continues straight up along the prominent vertical road. The next road encountered and crossed above this point is another horizontal road that intersects the prominent vertical road in the middle-right area. This is the second intersection. Finally, the route reaches the upper-right area of the image, where there is a large parking lot (the destination). This parking lot is located on a corner, bordered by roads on its right and top sides. The prominent vertical road runs along the left and bottom edges of this parking lot area. Although it is a large area, it does not appear to be a distinct "parking lot" that crosses another major road; rather, it is a large lot situated between two intersecting roads. Therefore, no additional intersections with other roads are gained by reaching this parking lot. Summarizing the intersections: * First intersection: horizontal road at middle-left.* Second intersection: horizontal road at middle-right.* Arrive upper-right parking lot area, but no additional road crossings beyond these two.</think> 2

Figure 11. Reasoning cases of RS-EoT-7B (Part 1).

Q: How many cars are in the left-turn lane?



Alright, I will reason in a self Q&A style and give the final reply. Start with a global observation to confirm the presence of a left-turn lane at the intersection, establishing the target lane's identity before counting. Is there a left-turn lane visible at the intersection? Let's look at the image. Yes, there is a left-turn lane visible at the intersection. It is the lane on the far left side of the road, marked with a white arrow pointing towards the upper left corner of the image. We have identified the left-turn lane. Next, determine whether any vehicles are present in that specific lane to set the base count before checking for additional cars. Is there at least one car positioned within the left-turn lane at the intersection? Let's look at the image. Yes, there is at least one car positioned within the left-turn lane at the intersection. I can see a dark-colored car in the leftmost lane, which is the left-turn lane, near the top of the image. Global observation confirmed a left-turn lane at the intersection. Targeted check indicated at least one car present within that lane. No conflicting cues or indications of an empty lane were observed. Final review finds no additional cars requiring counting.</think> 1

Q: What is the main land-cover type in this remote sensing image?



Alright, I will reason in a self Q&A style and give the final reply. Start with a global assessment to identify the single most dominant land-cover category by area. Determine if water bodies cover the largest area to guide subsequent focused checks. Does a large water body (river, lake, or sea) cover the largest area in the image? Let's look at the image. The image is primarily covered by dense green vegetation, which appears to be trees and bushes. There are also numerous small, irregular patches of lighter brown or greyish ground visible throughout the vegetation, which seem to be clearings or unpaved areas. Additionally, there are many residential buildings and paved roads. There are some very small, dark blue or greenish features, which could be swimming pools, located next to some of the buildings in the lower right and central-right portions of the image. However, these are very small in area compared to the vast expanse of vegetation. Therefore, no large water body such as a river, lake, or sea covers the largest area in the image. The largest area is covered by vegetation. Global observation indicates that vegetation covers the largest area, with no large water bodies and only small pools present. Final review finds no other land-cover type dominating.</think> Vegetation

Q: Describe this remote sensing image.



Alright, I will reason in a self Q&A style and give the final reply. Start with a broad global assessment to determine the overall scene type and guide subsequent focused questions. Is the scene predominantly urban/built-up? Let's look at the image. The scene contains a large stadium with a running track and a green field, multiple tennis courts, a basketball court, a parking lot with numerous cars, and many buildings with roads and paved areas. While there are green spaces and trees, a significant portion of the image is covered by man-made structures and infrastructure. Therefore, the scene is predominantly urban/built-up. From the global view, the scene appears urban with a prominent sports complex. Next, confirm the central anchor object to structure the caption. Is there a large stadium with a green field and a running track at the center of the image? Let's look at the image, yes, there is a large stadium with a green field and a running track at the center of the image. We have a global understanding: an urban scene centered on a stadium with sports facilities and parking. Next, confirm surrounding sports facilities for detailed spatial description. Are multiple tennis courts visible adjacent to the stadium? Let's look at the image. Yes, there are multiple tennis

courts visible adjacent to the stadium. They are located to the right of the stadium in the image. We have a global understanding and confirmed the stadium and adjacent sports facilities. Next, determine the parking arrangement to describe spatial flow and context. Is there a large parking lot with many cars immediately to the left of the stadium? Let's look at the image. Yes, there is a large parking lot with many cars immediately to the left of the stadium. We have identified an urban scene centered on a stadium with adjacent sports facilities and parking. To enrich the caption with architectural context, determine the predominant building type around the stadium. Are the surrounding buildings predominantly low-rise with flat roofs? Let's look at the image. Yes, the surrounding buildings appear to be predominantly low-rise with flat roofs. There are no visible indications of significant height or sloped/pitched roofs on the buildings. Global view shows a predominantly urban scene. Confirmed a central stadium with a green field and running track, adjacent sports facilities (tennis courts to the right), a large parking lot with many cars to the left, and a ring of low-rise buildings with flat roofs. Roads and paved areas are extensive; vegetation is secondary. No contradictions found; ready to deliver the caption.</think> A high-resolution urban scene centered on a multi-purpose stadium complex. At the heart of the image is a rectangular green playing field encircled by a red running track, with tiered spectator stands surrounding it. Immediately to the right of the stadium lie several tennis courts and a basketball court, set within paved aprons and bordered by paved roads. To the left of the stadium, a large parking lot packed with many cars is connected by a network of access roads. The area is densely built, with numerous low-rise buildings featuring flat roofs forming a continuous urban fabric around the sports facilities. Surfaces vary from dark asphalt and light concrete to red track surfaces and bright green turf, with trees and planted greenery lining pavements and interspersed between buildings, but vegetation is secondary to built-up areas and paved surfaces. The overall layout exhibits a clear contrast between the stadium's oval athletics track and the rectilinear arrangement of courts, parking, and buildings, all organized by a visible road grid.

Figure 12. Reasoning cases of RS-EoT-7B (Part 2).

Q: How many vessels are sailing in the image?



Alright, I will reason in a self Q&A style and give the final reply. Start with a global check to confirm the presence of a water body, which guides where vessels would appear. Is there a large water body visible in the image? Let's look at the image. Yes, there is a large water body visible in the image, occupying a significant portion of the lower and central areas. Shift focus to counting by spatial partition to efficiently determine the total number of vessels. How many vessels are visible in the left half of the image? Let's look at the image. I can see several vessels on the water. I will mentally divide the image vertically into two halves. In the left half of the image, I observe three vessels. These are long, narrow, dark-colored boats, each with a visible wake trailing behind them. In the right half of the image, I observe four vessels. These vessels are also long, narrow, and dark-colored, with visible wakes. Therefore, there are 3 vessels in the left half of the image. We have a global understanding and a partial count (3 in the left half). To compute the total, we need the count in the right half. How many vessels are visible in the right half of the image? Let's look at the image. I can see several vessels on the water. I'll divide the image vertically into two equal halves to count the

vessels in the right half. In the right half of the image, I can identify five vessels: 1. A long, dark vessel with a visible wake, located towards the bottom right. 2. Another long, dark vessel with a visible wake, positioned slightly above the first one and to the left. 3. A shorter, dark vessel with a visible wake, located further up and to the left from the second one. 4. A very small, dark speck in the water, located slightly above the third vessel and to the left. 5. Another very small, dark speck in the water, located further up and to the left from the fourth vessel. Therefore, there are 5 vessels visible in the right half of the image. Global scan confirms a large water area. Focused counts: 3 vessels in the left half and 5 in the right half, totaling 8. No contradictions detected; final review suggests no vessels near the vertical midline that would cause double counting. </think> 8

Q: Provide a detailed caption.

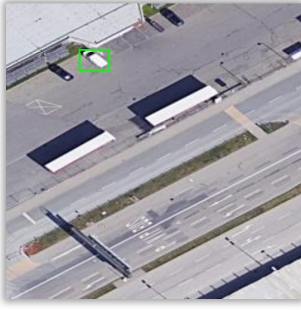


Alright, I will reason in a self Q&A style and give the final reply. Begin with global scene categorization to establish whether the landscape is predominantly urban, which guides subsequent focused questions on infrastructure, water, and land-cover patterns. Is the scene predominantly urban with dense building coverage? Let's look at the image. The scene is not predominantly urban with dense building coverage. Instead, it features large, light-colored sandy areas, several large triangular structures that appear to be pyramids, and a network of roads. There are also some scattered, smaller, darker structures, possibly related to the pyramids or other facilities, but these are not dense and do not constitute a predominantly urban environment. From the initial global view, the scene includes light sandy terrain, several large pyramids, and a road network with sparse darker structures. To craft a precise caption, first confirm the exact number of pyramids as a key scene element. How many large pyramidal structures are visible in the scene? Let's look at the image, I can see three large pyramidal structures. One is in the upper-middle section, another is in the lower-middle section, and a third is partially visible in the bottom-left corner. To enrich the caption with

environmental context, determine the dominant surrounding land cover beyond the pyramids and roads. Is the ground surface predominantly light-colored sand with broad sandy expanses? Let's look at the image, yes, the ground surface is predominantly light-colored sand, with broad expanses of it covering most of the visible area. To enrich the caption with environmental context, confirm whether any water features are present, which would significantly affect scene description. Is any water body visible in the scene? Let's look at the image, I have carefully examined the entire scene, and I do not see any visible water bodies. To enrich the caption with contextual infrastructure, verify whether there are additional man-made structures beyond the pyramids and roads, which helps describe the site's layout and land use. Besides the pyramids and roads, are there any other notable man-made structures visible? Let's look at the image. Yes, besides the pyramids and roads, there are other notable man-made structures visible. In the upper right portion of the image, there is an area with numerous small, dark, rectangular shapes arranged in rows. These appear to be buildings or paved areas. Some of these are larger, suggesting they could be facilities or compounds. This area is adjacent to what looks like an unpaved or dirt track. Further down, towards the middle right, there's a larger, irregularly shaped complex of darker material, possibly debris or construction refuse, located near some sparse vegetation. In the bottom right corner, there's a small, bright, rectangular object that could be a vehicle or a small piece of equipment. Global view shows a non-urban desert scene dominated by light sand, three large pyramids, and a road network; detailed checks confirm three pyramids (one upper-middle, one lower-middle, one partial bottom-left), broad sandy expanses, no water bodies, additional man-made clusters of small dark rectangular structures (upper right), an irregular darker refuse/ debris area (middle right), sparse vegetation, and a bright rectangular object (bottom right). All key regions reviewed and consistent; ready to provide the caption. </think> A remote desert landscape dominated by light tan sand dunes and broad, open terrain, punctuated by three large pyramidal structures: one in the upper-middle, one in the lower-middle, and a partial third at the bottom-left edge. A network of roads and unpaved tracks weaves around the pyramids, linking them to clusters of small, dark rectangular buildings and paved areas in the upper-right portion of the scene. The area also contains an irregular, darker accumulation of refuse or debris near some sparse vegetation on the right, with a few isolated vehicles or small pieces of equipment visible, including a bright rectangular object in the bottom-right corner. No water bodies are present, and the surrounding ground is largely unvegetated, with strong sunlight textures and sharp shadows highlighting the pyramids and structural clusters.

Figure 13. Reasoning cases of RS-EoT-7B (Part 3).

Q: Locate the white car in the image. Return the coordinates as "[x1, y1, x2, y2]".



Alright, I will reason in a self Q&A style and give the final reply. Start with a global check to understand the scene layout and identify likely regions where a car might appear, such as roads or parking areas. Is there a paved road or parking area visible in the image? Let's look at the image. Yes, there are several paved areas visible. There's a large paved area in the upper left with a white car parked on it, and multiple paved roads with lane markings running diagonally across the lower and middle parts of the image. We have identified a large paved area in the upper-left where a white car is likely parked. Next, confirm the car's presence in that area. Is there a white car parked on the large paved area in the upper-left quadrant? Let's look at the image. Yes, there is a white car parked on the large paved area in the upper-left quadrant of the image. Global observation revealed paved roads and a large paved area; focused observation confirmed a white car parked on the upper-left paved area. No conflicting cues found upon final review; coordinates will be returned in a self Q&A style.</think> [128,81,177,115]

Q: Locate the swimming pool in the image. Return the coordinates as "[x1, y1, x2, y2]".



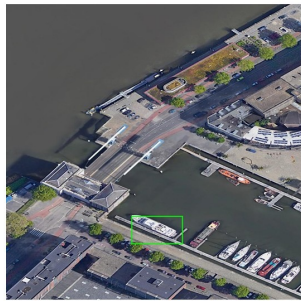
Alright, I will reason in a self Q&A style and give the final reply. Start with a global scan to detect any prominent water-like area, which is a common high-level cue for pools. This broad check guides subsequent focused localization. Is there any noticeable blue or turquoise area with smooth, curved boundaries visible in the image? Let's look at the image, yes, there is a very noticeable blue area with smooth, curved boundaries visible in the image. It is a swimming pool located in the upper-middle portion of the image. We have a global indication of a blue, curved-boundary area likely being the pool. To confirm precise localization for coordinates, first verify that there is only one such area to avoid ambiguity. Is there exactly one blue area with smooth, curved boundaries in the image? Let's look at the image, I can see a prominent blue area with smooth, curved boundaries. This area is a swimming pool. I do not observe any other blue areas with smooth, curved boundaries in the image. Global observation identified a single blue, smooth-boundary area; focused checks confirmed it is a swimming pool with curved edges; no conflicting cues found; final review complete.</think> [369,203,538,297]

Q: Locate the train in the image. Return the coordinates as "[x1, y1, x2, y2]".



Alright, I will reason in a self Q&A style and give the final reply. Start with a global check to see if any train-like object exists in the scene before narrowing down its location. Is there at least one train visible anywhere in the image? Let's look at the image. Yes, there is at least one train visible in the image. It is located on the far right side, towards the top, on the railway tracks. A portion of a train, likely its roof, can be seen extending into the image frame from the right edge. Global observation confirmed the presence of a train; it was noted near the top-right along the tracks. No conflicting cues found upon quick review. Ready to provide the concise location.</think> [753,127,796,309]

Q: Locate the largest cruise ship in the image. Return the coordinates as "[x1, y1, x2, y2]".



Alright, I will reason in a self Q&A style and give the final reply. Start with a global scan to confirm the presence of maritime context, then narrow to locating large ship-like vessel(s) in the main water area. Is there a large water body visible in the image? Let's look at the image. Yes, there is a large water body visible in the image, occupying a significant portion of the left and central areas. From the global scan, a large water body is present. Next, I need to localize large ship-like vessels to identify potential candidates for the largest cruise ship. Are there any large ship-like vessels visible on the water? Let's look at the image. Yes, there are several large ship-like vessels visible on the water. Specifically, in the lower central part of the image, there is a very prominent, long, white vessel docked alongside a pier. It has a distinct hull and a superstructure, making it appear like a large yacht or a private vessel. Further down and to the right on the water, there's a cluster of smaller, more traditional boat-like shapes, which appear to be barges or working vessels, but one of them is quite long and somewhat rectangular, resembling a barge. In the upper left portion of the water, there's a long, narrow structure, which appears to be a bridge or a drawbridge, extending over the water. It's a large, man-made structure, but it's a bridge rather than a ship. To identify the largest cruise ship, I will first confirm whether the prominent long white vessel in the lower center is a passenger-carrying cruise ship rather than a barge. Does the long white vessel in the lower center have multiple passenger cabins visible on its deck? Let's look at the image. The long white vessel in the lower center of the image is a large yacht. On its deck, multiple passenger cabins are visible. Global scan confirms a large water body with several ship-like vessels. Focused inspection identifies a prominent long white vessel with multiple cabins in the lower center, consistent with a cruise ship. No larger candidate observed; final checks complete.</think> [341,575,476,647]

Figure 14. CReasoning cases of RS-EoT-7B (Part 4).

Q: Locate **the truck** in the image. Return the coordinates as "[x1, y1, x2, y2]".



Alright, I will reason in a self Q&A style and give the final reply. Begin with a global check to confirm the presence of a truck before localizing it. Is there at least one truck visible in the image? Let's look at the image. Yes, there is at least one truck visible in the image. It is located on the road in the bottom left portion of the image, appearing as a large white and red vehicle. Presence of a truck is confirmed. To provide precise localization for the coordinates, verify whether there is exactly one truck in the image so that global and local positions align. Is there exactly one truck visible in the image? Let's look at the image. Yes, there is exactly one truck visible in the image. It is located on the road in the bottom left portion of the image. Global observation confirmed presence of a truck; focused check verified there is exactly one truck visible. Final review finds no additional trucks elsewhere. Ready to provide the coordinates.</think> [56,594,154,650]

Q: Locate **the taxiing plane** in the image. Return the coordinates as "[x1, y1, x2, y2]".



Alright, I will reason in a self Q&A style and give the final reply. Start with a global check to confirm the presence of airplanes before focusing on taxiway localization. Are there any airplanes visible in the image? Let's look at the image. Yes, there are airplanes visible in the image. I can see four distinct airplanes. We have confirmed multiple airplanes are present. Next, determine whether one is on a taxiway rather than at a terminal gate, which is necessary to identify the "taxiing plane." Is there an airplane positioned on a taxiway (not at a terminal gate)? Let's look at the image. Yes, there is an airplane positioned on a taxiway. The large paved area where the airplanes are located is a taxiway, and there are no visible terminal gates in the image. We identified multiple airplanes and confirmed one is on a taxiway. To provide precise coordinates, we should locate the taxiway-facing nose of that specific plane. Is the airplane on the taxiway oriented with its nose pointing toward the top edge of the image? Let's look at the image. There are four airplanes visible. The airplane on the far left is oriented with its nose pointing towards the top-left corner of the image. The second airplane

from the left is oriented with its nose pointing towards the right-middle of the image. The third airplane from the left is oriented with its nose pointing towards the bottom-right of the image. The airplane on the far right is oriented with its nose pointing towards the top-right corner of the image. Therefore, only two of the airplanes are oriented with their noses pointing toward the top edge of the image. We have multiple airplanes on a taxiway, with at least two oriented toward the top edge. To uniquely identify the "taxiing plane," I will confirm which one is actively moving by checking for a trailing wake. Is there a plane showing a visible wake trailing behind it, indicating movement? Let's look at the image. I am examining all four airplanes visible in the image. I do not see any visible wake trailing behind any of the planes. All the airplanes appear to be stationary on the tarmac. There seems to be a mismatch: earlier indications suggested at least one plane is on a taxiway, but the orientation check showed most noses aren't toward the top edge, and no wake was seen. To resolve this, I will verify whether any plane's nose points toward the bottom edge, which would indicate taxiing. Is any airplane oriented with its nose pointing toward the bottom edge of the image? Let's look at the image. Yes, there is one airplane oriented with its nose pointing toward the bottom edge of the image. This airplane is located in the bottom right portion of the image. Global view confirmed multiple airplanes on a taxiway. Detailed checks showed most noses aren't toward the top edge, but one plane in the bottom-right has its nose pointing toward the bottom edge, consistent with taxiing. Final review finds no conflicting cues.</think> [447,490,583,589]

Q: Locate **the smaller ship** in the remote sensing image. Return the coordinates as "[x1, y1, x2, y2]".



Alright, I will reason in a self Q&A style and give the final reply. Start with a global assessment to understand the scene layout and identify whether water dominates, which guides where ships would appear. Is the majority of the image covered by water? Let's look at the image. The majority of the image is covered by a dark green, textured surface that appears to be water. Yes, the majority of the image is covered by water. With the global scene confirmed as mostly water, next I need to verify that ships are present to locate the smaller one. Are there multiple ships visible on the water surface? Let's look at the image. Yes, there are multiple ships visible on the water surface. I can clearly see two distinct ships. Global scene is water with two ships. To identify which is smaller, I will compare their sizes directly. Is the ship in the upper-left part of the image smaller than the ship in the lower-central part? Let's look at the image. The ship in the upper-left part of the image is smaller than the ship in the lower-central part. Global view shows a mostly water scene with two ships. Focused comparison confirms the upper-left ship is smaller than the lower-central one. No contradictions observed; final check complete.</think> [108,58,154,187]

Figure 15. Reasoning cases of RS-EoT-7B (Part 5).